SOME PROPERTIES OF VELOCITY FIELDS IN THE SOLAR PHOTOSPHERE*

V: *Spatio-Temporal Analysis of High Resolution Spectra*

FRANZ-LUDWIG DEUBNER
Fraunhofer-Institut, Freiburg i.Br., F.R.G.

(Received 25 July, 1974)

Abstract. Series of high resolution spectrograms taken simultaneously in three spectral regions were recorded with a lambda meter and subjected to a statistical analysis of the fluctuations of Doppler shift and brightness.

(1) The 5-min oscillations are confirmed to be 'evanescent' waves. Their horizontal wavelengths range from 9″ to 15″ and probably still larger values.

(2) Horizontal sound waves (Lamb waves) are only of minor importance in the photospheric velocity field.

(3) Vertically propagating sound waves are observed and are used to establish a geometrical height scale. The horizontal wave numbers of these sound waves cover a wide range including the scales of both the 5 min oscillations and the granular convection.

(4) The inversion of the granular brightness pattern at higher photospheric levels is confirmed for wavenumbers smaller than 8 Mm^{-1}. At $k \approx 10$ Mm^{-1}, however, the correlation of brightness and blue shift observed in the photosphere holds also in lines originating as high as Na I(D_1). This statistical result is related to structures directly visible in spectrograms.

1. Introduction

During the past decade considerable efforts have been made, both observationally and theoretically, to investigate the macroscopic motion fields of the solar atmosphere and the 300-s oscillations in particular. It is generally accepted that a proper understanding of the role of wave motions in the process of chromospheric heating and also of the observed oscillatory and quasioscillatory phenomena by themselves are fundamental constituents of any theory of the solar atmosphere.

The most comprehensive kind of analysis of these phenomena is made possible through spatio-temporal Fourier decomposition of the observed motions which allows a comparison of the velocity field with the linear wave modes possible in a homogeneous stratified atmosphere by means of diagnostic (k, ω) diagrams. The papers by Mein (1966), based on the excellent material collected by Evans and Michard (1962), by Edmonds and Webb (1972) and Frazier's (1968) work summarize most of the information available at that time about velocity fields at different levels of the solar atmosphere. More recently Stix and Wöhl (1974) have extended the observations to positions on the solar disk other than the center (where horizontal sound waves cannot be detected).

The observations discussed in this paper were intended to help in answering some

* Mitteilung aus dem Fraunhofer Institut Nr. 131.

Solar Physics **39** (1974) 31–48.

of the intriguing questions which characterize the discussion about oscillatory velocity fields:

Excitation mechanisms: Are the 5-min oscillations locally excited by some kind of convective pistons (granules or otherwise), or do they result from an oscillatory instability of the upper layers of the solar body as a whole?

Scale: Which one of the different theories about the oscillatory phenomena predicting various typical horizontal wavelengths in the range from ≈ 1.5 Mm (Thomas, 1972) to 20 Mm and more (Wolff, 1973) is sustained by observation?

Propagation: Are there wave modes present which propagate vertically, or horizontally? Are there dynamic processes detectable which contribute substantially to the chromosphere – corona energy balance?

In dealing with this controversial topic we cannot avoid mentioning again some facts or conclusions which have been published already. However, we feel that in several instances the strong observational argument now available will be helpful in settling the controversial matters.

2. Observations

The study of previous publications on the same subject reveals that very high resolution of the observations both in space and time is equally important as sufficient extension of the data in both coordinates, or, speaking in terms of Fourier transforms: a wide spectral window is essential in any attempt to answer some of the questions mentioned above. Most photo-electric observations available suffer from small sampling rates, low spatial resolution, and even more from the fact that observations made in only one spectral line yield only little information about the height dependence of the phenomena observed. We therefore decided that the present study should be based entirely on photographic spectra.

The observations were collected on September 6 and 8, 1971 with the echelle spectrograph of the vacuum tower at Sacramento Peak Observatory. Three spectral regions were recorded simultaneously on 70 mm film. 3-s exposures were made at 6-s intervals. This relatively short interval was chosen in order to enhance the statistical stability of the results and to provide sufficient temporal resolution for impulsive events. Table I gives the spectral lines used in this study and the relevant spectrographic data. Table II summarizes the geometric scale factors.

TABLE I

The Spectral lines used in this study

λ	Ident.	EP(eV)	EW(mÅ)	Lin. disp. (mm Å^{-1})	Band-pass (Å)
5380.32	C I	7.68	26	12.0	0.20
5382.28	–	–	23	12.0	0.20
5383.38	Fe I	4.31	204	12.0	0.12
5895.94	Na I(D_1)	0.00	564	10.9	0.14
6562.81	Hα	10.20	4020	9.8	0.40

TABLE II

The geometric scale factors

	(mm)	(arcsec)
Solar image size	537.5	1908
Effective slit length	63	224
Slit width	0.1	0.355
Scan interval	0.075	0.266
Scan element	0.1×0.1	0.355×0.355

Slit jaw pictures in white light and K (0.6 Å) were obtained simultaneously with the spectra, thus providing a straightforward check of the instrumental guiding and a means of recognizing regions of solar 'activity' on the slit.

The total duration of each series of exposures was 32 min, yielding 320 single spectra in each wavelength region. The spectrograph slit was aimed at the disk center on September 6 and at a distance from the center corresponding to $\mu = 0.8$ on the central meridian on September 8. The slit was always oriented parallel to the solar equator in order to minimize the effects of solar rotation and foreshortening. The solar atmosphere was 'quiet' in the regions recorded.

The seeing conditions were extraordinarily good and stable during the observations: It is possible to identify without difficulty almost any chosen granular fine structure on any frame in a series of consecutive spectra. During the observations one was able to follow easily the development of single granules on the TV white light slit jaw monitor. The rms granular velocities measured on these spectra (Deubner, 1974) are unusually high.

2.1. Data reduction

The great amount of photographic material collected in the way described above made it necessary to use relatively quick procedures for photometry and data reduction. A recording Doppler comparator (lambda meter) was used to measure the line displacements and transparencies in those parts of the line profiles which were transmitted to the comparator. Neglecting all detailed information from the line profiles, only these two quantities were recorded on magnetic tape.

Each scan (along the spectral line) consists of 759 points spaced at intervals of 0.″266. The height of the line segment admitted to the comparator is approximately equal to the spacing of the points, the total slit width (spectral band pass) used with the different spectral lines is given in the last column of Table I. The passbands fed to the comparator are not separated by a central stop. A reflecting prism divides the exit slit into two equal adjacent spectral bands with half the width given in Table I. Two hairlines produced on the spectra by the spectrograph slit served as a reference for the positioning of the records.

Preliminary data processing included the following steps:

Let

$$\left.\begin{matrix} D_0(i,j) \\ T_0(i,j) \end{matrix}\right\} \quad \begin{matrix} i = 1, M \\ j = 1, N \end{matrix} \qquad \begin{matrix} M = 759 \\ N = 320, \end{matrix} \tag{1}$$

be the raw data, recorded with the lamda meter, D standing for line displacement and T for transparency.

(1) Data from a few spectrograms with major photographic defects were replaced by interpolated data,

$$\left.\begin{aligned} D_0(i,j) &= 0.5\,(D_0(i,j-1) + D_0(i,j+1)) \\ T_0(i,j) &= 0.5\,(T_0(i,j-1) + T_0(i,j+1)) \end{aligned}\right\} i = 1, M. \tag{2}$$

(2) Line displacements were converted to velocities in m s^{-1},

$$D_0(i,j) \rightarrow V_0(i,j) \begin{cases} i = 1, M \\ j = 1, N. \end{cases} \tag{3}$$

(3) The gaps produced by the hairlines were filled with data interpolated linearly between the border points of the gaps in both sets of data.

(4) Temporal averages

$$\bar{V}(i) = \frac{1}{N} \sum_{j=1}^{N} V_0(i,j) \quad \text{and} \quad \bar{T}_0(i) = \frac{1}{N} \sum_{j=1}^{N} T_0(i,j) \tag{4}$$

were used to correct the data for spectral line curvature and for deviations of the parallelism of the slit jaws.

The line curvature was approximated by a second order polynomial $\bar{V}_1(i)$ fitted through $\bar{V}_0(i)$, whereas the reference curve for transparency $\bar{T}_1(i)$ had to be constructed from 23-point running means through $\bar{T}_0(i)$:

$$\left.\begin{aligned} V_1(i,j) &= V_0(i,j) - \bar{V}_1(i) \\ T_1(i,j) &= T_0(i,j) - \bar{T}_1(i) \end{aligned}\right\} \begin{aligned} i &= 1, M, \\ j &= 1, M. \end{aligned} \tag{5}$$

(5) Taking the spatial averages

$$\begin{aligned} \bar{V}_2(j) &= \frac{1}{M} \sum_{i=1}^{M} V_1(i,j), \\ \bar{T}_2(j) &= \frac{1}{M} \sum_{i=1}^{M} T_1(i,j), \end{aligned} \tag{6}$$

further corrections were applied for changing brightness of the solar image due to increasing elevation and irregularities of the exposures and for the relative positioning of the spectral line in the lambda meter:

$$\left.\begin{aligned} V_2(i,j) &= V_1(i,j) - \bar{V}_2(j) \\ T_2(i,j) &= T_1(i,j)/\bar{T}_2(j) \end{aligned}\right\} \begin{aligned} i &= 1, M, \\ j &= 1, N. \end{aligned} \tag{7}$$

(6) The rate of continuous drift of the solar image parallel to the slit was determined independently from analogue records of the spectra and from the K-line filtergrams. Incidentally, it appeared that the drift was only partly caused by solar rotation, a nearly equal amount of drift being introduced by a slowly increasing deviation of the guiding system. Fortunately, this deviation also ran parallel to the spectrograph slit during both observations.

The drift rates determined empirically are one step (0".266) in 48 s on September 6 and one step in 60 s on September 8. Considering the likeliness of image excursions up to 0".266 due to seeing we did not compensate the slow drift of the image by linear interpolation, but rather corrected the i-indices of the data arrays in appropriate intervals.

(7) The spatial index $i'=1, M'$ with $M'=720$ now indicates solar coordinates, and true temporal averages can be computed:

$$\bar{V}_2(i') = \frac{1}{N}\sum_{j=1}^{N} V_2(i', j); \quad \bar{T}_2(i') = \frac{1}{N}\sum_{j=1}^{N} T_2(i', j), \tag{8}$$

and extracted from the data:

$$\begin{aligned} V_3(i', j) &= V_2(i', j) - \bar{V}_2(i'), \\ T_3(i', j) &= (T_2(i', j) - \bar{T}_2(i'))/\bar{T}_2(i'). \end{aligned} \tag{9}$$

If used in connection with the slit jaw filtergrams, the temporal averages provide further useful information on the position of long lived structures (network boundaries, faculae etc.) which are covered by the spectrograph slit.

The final 320 by 720 point data arrays which represent spatio-temporal fluctuations of the velocity and brightness in four different layers of the solar atmosphere were then subjected to one- and two-dimensional Fourier transforms by using standard FFT techniques (cf. Edmonds and Webb, 1972).

Under the assumption of two-dimensional isotropy it is possible to convert the one-dimensional wavenumber spectra obtained from FFT analysis to radial wavenumber spectra, using the integral transform given by Uberoi (1955),

$$P(k) = -k \int_{k_x=k}^{\infty} \frac{\mathrm{d}P(k_x)/dk_x}{\sqrt{k_x^2 - k^2}}\,\mathrm{d}k_x, \tag{10}$$

modified to yield the correct power distribution per unit wave number. This transform does not produce any negative power at large wavenumbers, which usually occurs when the Hankel transform is computed from the auto-covariance function. We therefore adopted this procedure for ali wavenumber spectra presented in this paper.

Phase spectra can be obtained either from one-dimensional Fourier-transforms thereby neglecting all spatial information, or from two-dimensional transforms in k and ω. The latter way offers the possibility of determining phases as a function not only of the temporal period but also as a function of the size of the structures involved, by averaging the phase only in the k, ω regime of interest. 'Coherence' values were obtained together with the 'phase' by either smoothing (by averaging) exclusively with respect to wavenumber k, or (in the case of one dimensional k-spectra) by averaging with respect to time t rather than frequency ω. Since in the two-dimensional phase spectra no significant dependence of the vertical phase velocities on the horizontal wave number has been observed, the 'coherence' spectra shown in the figures

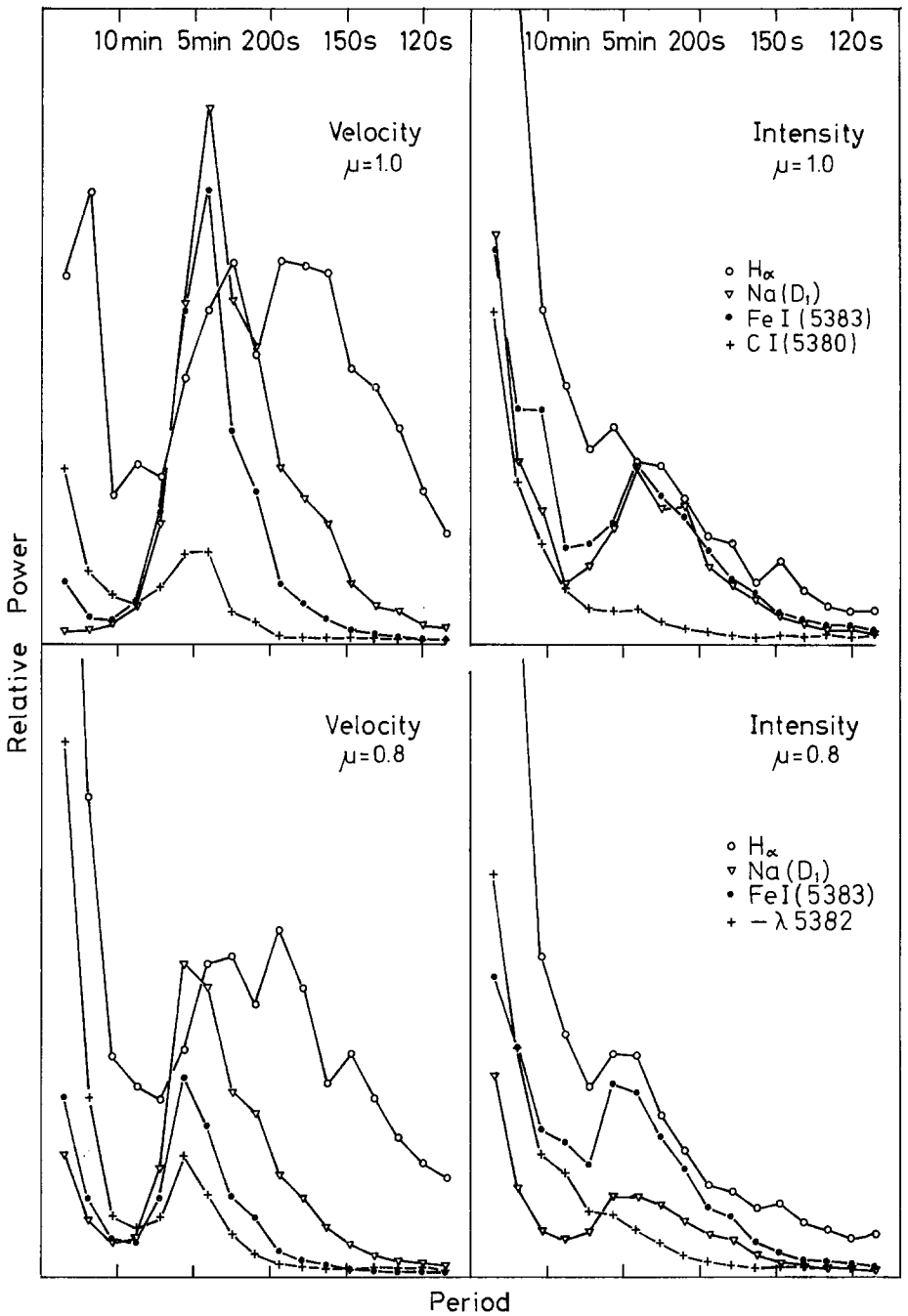

Fig. 1. Frequency spectra of velocity and intensity fluctuations measured simultaneously in several Fraunhofer lines at two position on the disk. The kinetic power spectra of Hα have been scaled down by a factor of 0.2 relative to the other lines.

reflect the statistical stability of the phase estimates rather than the spatial coherence of the wavetrains. (See also Edmonds and Webb (1972a) for a discussion of 'coherence' spectra.)

3. Results

One-dimensional ω-spectra are presented in Figure 1 for four different spectral lines and two positions on the disk, both of brightness and velocity fluctuations.
Some particular features can be seen more easily here than in the two-dimensional presentation of the same data discussed later on.

(1) The position of the principle power peak connected to the 5-min oscillations moves only marginally from the photospheric values (period $T \approx 300$ s) toward shorter periods in the lines representing the higher layers ($T > 240$ s). Additional power in the sodium line and even new maxima in Hα at higher frequencies far beyond $3 \times 10^{-2}\ s^{-1}$ shift the mean period to $T \approx 180$ s. It appears, however, from the k, ω spectra that these maxima rather belong to running acoustical waves and are only partly related to the 5-min oscillations.

(2) With regard to intensity fluctuations neither the power spectra of the low photospheric layers (C I) nor those of Hα exhibit a major response to the prominent velocity fluctuations in the 5-min domain. In the photosphere this lack of response is already known from earlier observations and has been explained as a result of the short thermal relaxation time (Stix, 1970) which makes the oscillations almost

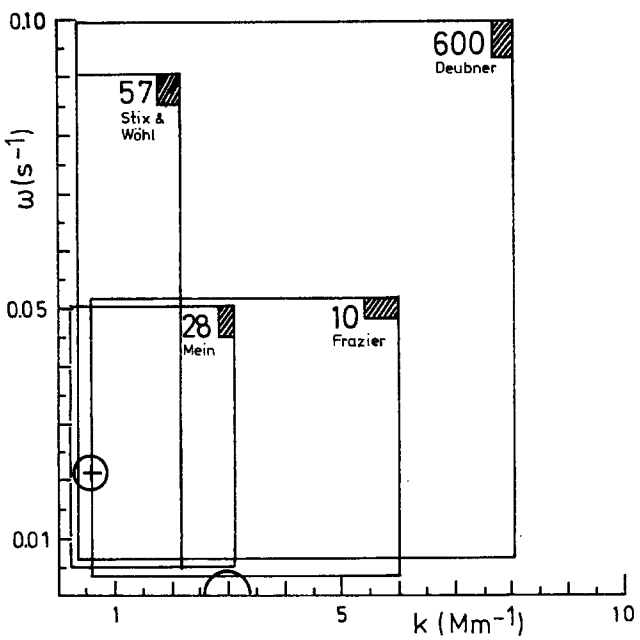

Fig. 2. Spectral window (large rectangle), spectral resolution element (shaded area), and number of 'degrees of freedom' valid for the k, ω diagrams shown in Figures 3 to 6 in comparison with the observational limitations of some previous authors. The loci of maximum power of the 5-min oscillations (full circle) and granular fluctuations (half circle) are indicated.

isothermal. In Hα the relaxation time is much longer. Nonetheless the response is missing, presumably because in Hα the source function is controlled by the radiation field of extended lower layers to such a degree that a response to local density fluxtuation cannot be observed.

(3) Recently, the existence of long period oscillations with periods of about 20 min has been investigated both theoretically (Wolff, 1972a) and by observations (Fossat and Ricort, 1973, and Deubner, 1972). The spectra shown here indicate that there are no peculiar long periods present. The power increases rather continuously and merges into the strong low frequency tail connected to the convective motions.

This result is fully confirmed by some new photoelectric measurements with the Capri magnetograph providing much higher frequency resolution and statistical stability than the present results have in the relevant k, ω domain. These series of

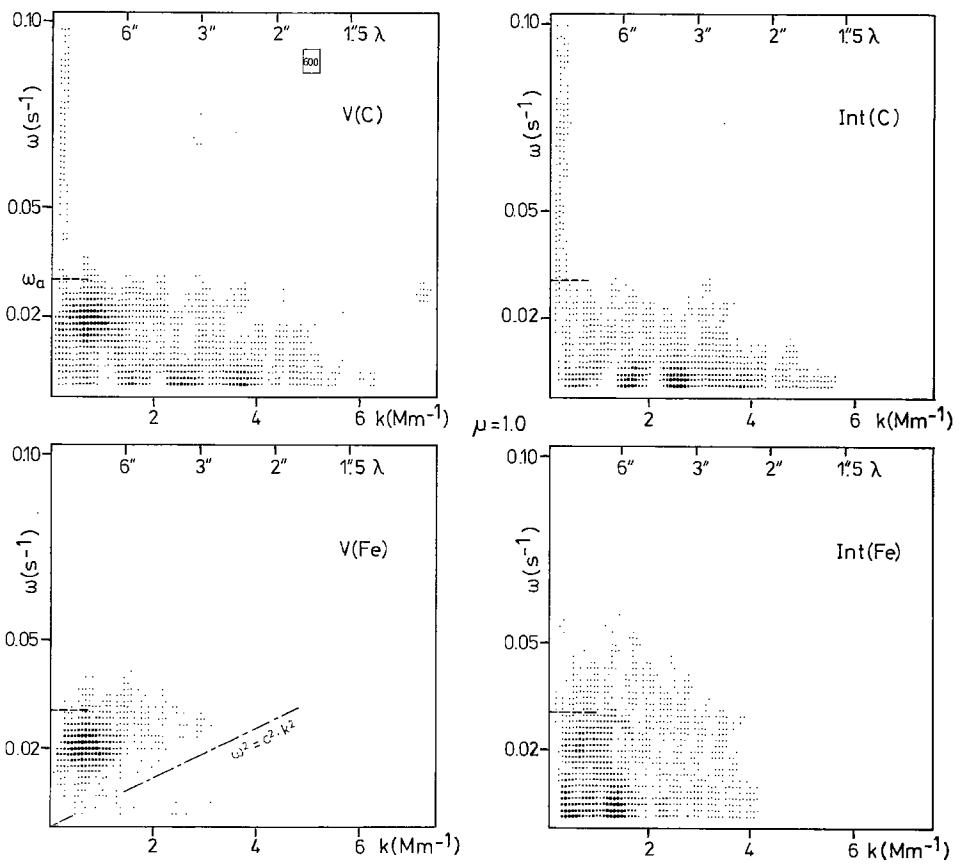

Fig. 3.

Figs. 3–6. Diagnostic (k, ω) diagrams of velocity and intensity fluctuations of photospheric and chromospheric Fraunhofer lines at two positions on the disk. The power levels as indicated by six different dot sizes correspond to 2.8 %, 11.1 %, 25.0 %, 44 %, 69 % and 100 % of maximum power. The acoustic cut off frequency is marked by a dashed line segment. The origin of the power visible in some of the diagrams at high frequencies and low wave numbers is instrumental.

automatically guided observations in various spectral lines, each one extending several hours, failed to show any particular oscillations at low frequencies.

Two-dimensional k, ω spectra (diagnostic diagrams). In Figures 3 to 6, line printer plots of the frequency-wavenumber spectra are reproduced, which are based on the material described in the preceding chapter. The data necessary for appreciating the statistical significance of the power distributions are given in Figure 2 and explained in the caption. In particular the spectral window (spatial as well as temporal resolution and resolution in Fourier space) pertinent to the present analysis is compared with the windows of spectra published by other authors. The influence of seeing becomes substantial only close to the right hand border of the spectra, where the power (with the exception of the C I measurements) is far below the 3% of maximum power contour which terminates the plotter printing. Figure 2 also illustrates to what extent the relevant features of the k, ω diagram have been covered by the observations.

Since diagnostic diagrams of the solar atmosphere have been discussed in detail already by several of the authors mentioned before, here only the most important

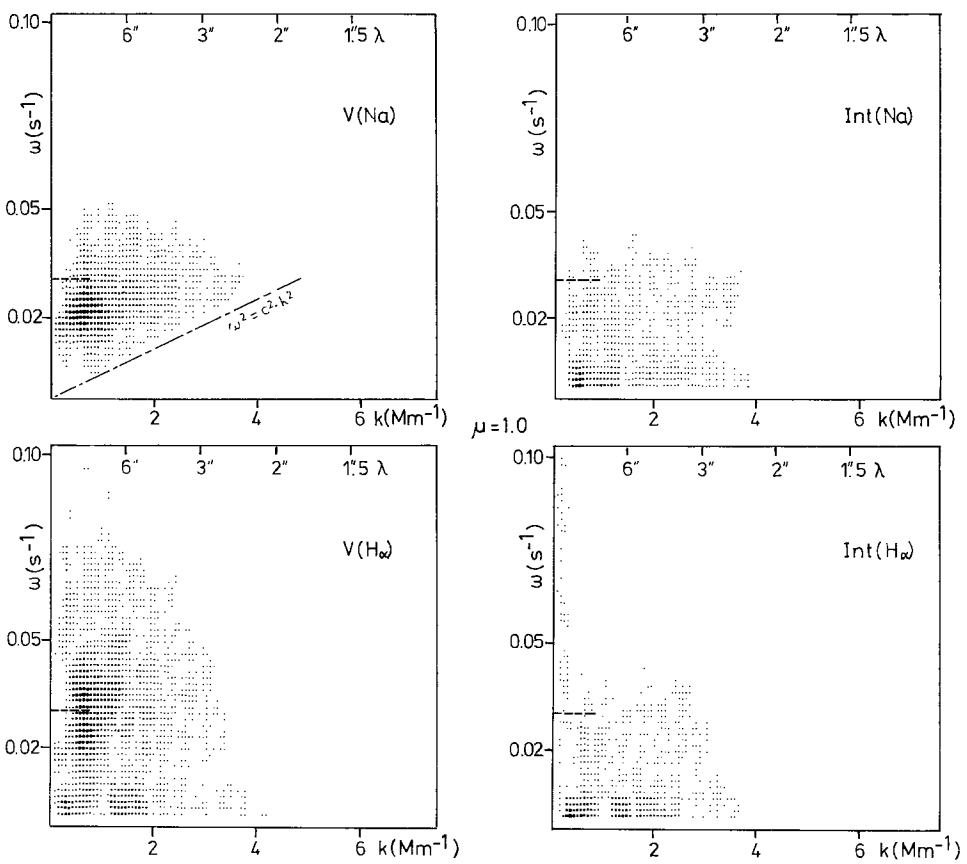

Fig. 4.

observations will be summarized, but we shall give a more detailed account of some properties, which were not reported or not well established before.

Low frequencies (ω)

In the ω-domain close to the k-axis a concentration of power is observed in the photospheric spectra (C I) towards lower frequencies at almost all wavenumbers with the exception of one conspicuous gap at $k \approx 1$ Mm^{-1}. Clearly, the convective velocity fields of the photosphere can be recognized in this part of the diagnostic diagram. In particular, we identify the area both of supergranulation at $k < 1$ Mm^{-1} (which can be better detected by means of the intensity fluctuations at the disk center because of the small amplitude of the vertical motions) and of the '5″-granulation' at $k \approx 1.5$ Mm^{-1}. In one-dimensional k spectra of low resolution the latter does not appear well separated from the 5-min oscillations and it is therefore easily confused with them. The k, ω diagram proves its convective origin beyond doubt.

In the range from 2 to 5 Mm^{-1} there are quite a number of peaks, the position of which changes from one observation to another as comparisons with previous authors

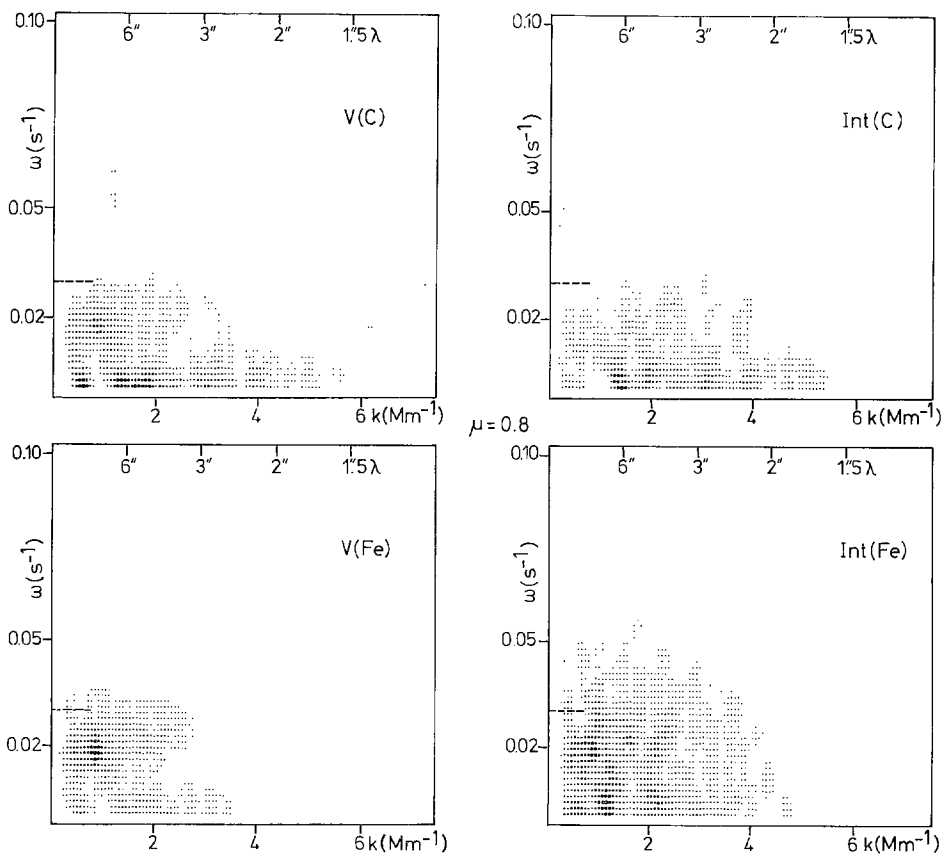

Fig. 5.

(cf. Mattig and Nesis, 1974) reveal. Yet the centers of gravity of all the power distributions published coincide very closely at $k = 3.0\ \mathrm{Mm}^{-1}$. (A more detailed discussion of the statistical significance of the wavenumber spectra of granules based on the same observations has been published recently by the present author, Deubner, 1974).

Exactly at this position a protrusion of the power distribution to higher frequencies is observed, preferentially at the disk center which signals the presence of genuine gravity waves excited by single granules. This observation corroborates the theoretical finding (Clark and Clark, 1973) that gravitational waves just cannot be avoided in the photosphere. However, this domain of the power spectrum is apparently in no way linked to the 5-min oscillations.

5-MIN OSCILLATIONS

The Figures 3 to 6 demonstrate that the spectral resolution achieved in k with due consideration of the statistical stability is just marginally sufficient to establish the mean wavenumber of the 5-min oscillations. The maximum of the energy distribution is found at wavenumbers between 0.6 and $1.0\ \mathrm{Mm}^{-1}$ (9″–15″). There is, however,

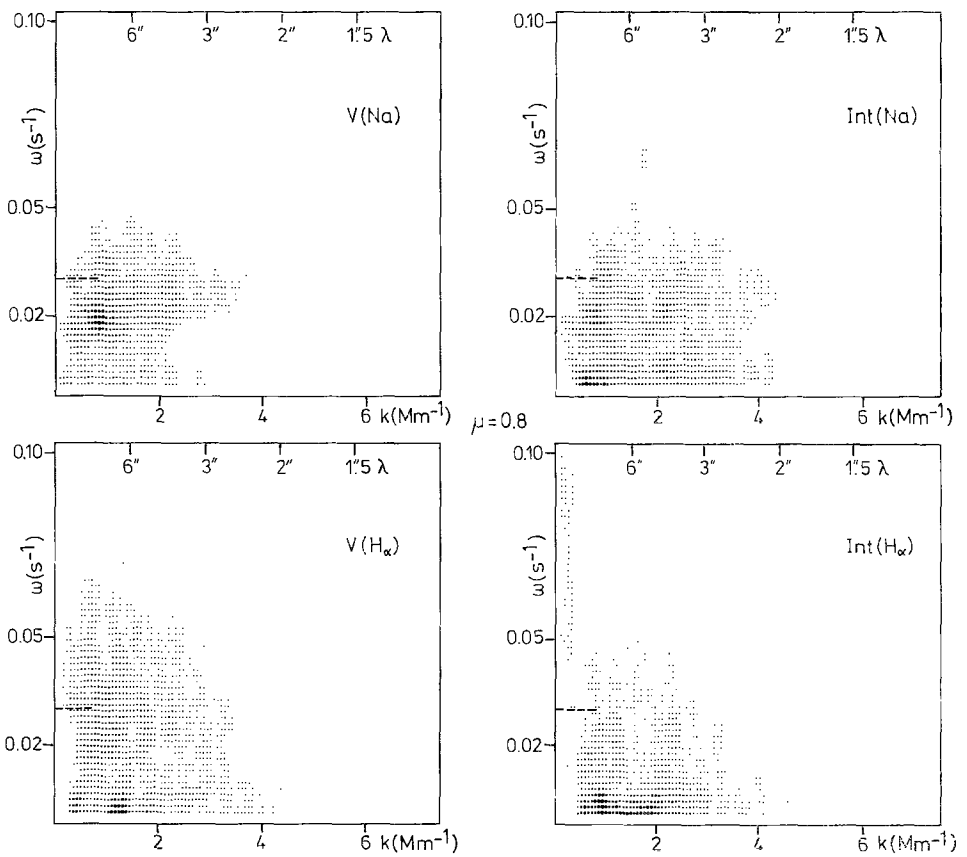

Fig. 6.

still considerable energy present in much smaller wavenumbers near $k=0.3$ Mm^{-1}, confirming earlier estimates given by Tanenbaum *et al.* (1969), Deubner (1972), and Fossat and Ricort (1973), who all report the occurrence of still larger wavelengths in the oscillatory velocity field.

A direct physical relationship between the 5-min oscillations and either granulation or supergranulation appears now to be ruled out definitively because of the diverging ranges of the wavenumbers involved.

With regard to frequency the 5-min oscillations occupy an area in the k, ω plane where neither sound waves nor gravity waves do propagate. This is consistent with models which predict the observation of forced motions of the atmosphere which follow the selfexcited oscillations produced in subphotospheric layers.

Vertical sound waves

Propagating acoustical waves occurring at frequencies higher than the acoustical cutoff frequency $\omega_a=0.03$ s^{-1} can be seen in all layers observed and become increasingly important with increasing height of the line-forming layer. A simple relationship with the low frequency phenomena is not apparent from the diagrams. However, there is in all layers a large amount of energy concentrated in the range of granular wave numbers, whereas in the higher layers the 5-min oscillations develop a prominent 'high frequency tail' of their own. Accordingly, the additional power peaks observed in chromospheric ω spectra mentioned before are composed of contributions from different noncoherent sources.

We would like to mention here an observation made of single prominent small scale disturbances which propagate through the whole visible atmosphere. During such an event (see Deubner, 1973) propagating sound waves (among other wave modes) are shown to be produced in the Fe I and NaD_1 forming layers by the convective overshoot of an impulsive (exploding) granule appearing first at the photospheric level, as predicted some years ago by Meyer and Schmidt (1967) in the framework of their oscillations model. – In the spectra in Figure 3 to 6 there is a gradual decrease of power from evanescent to propagating sound waves as in the one dimensional ω spectra.

Horizontal sound waves (Lamb waves)

The diagrams of the two medium layers (where the 5-min oscillations are particularly prominent) document nicely the total absence of vertical motions in the area traversed by the line $c^2=\omega^2/k^2$ defining the locus of horizontal sound waves. However, the contribution of Lamb waves to the total power is rather small also at other positions on the disk ($\mu=0.8$ in this paper), as reported already by Stix and Wöhl (1974).

Phase spectra. In order to achieve a higher statistical stability and at the same time to make the spectra more readable, the phase (and coherence) has not been plotted two dimensionally as functions of k and ω, but rather have been drawn as a function of one of the coordinates only, after averaging the values in the other, for the most

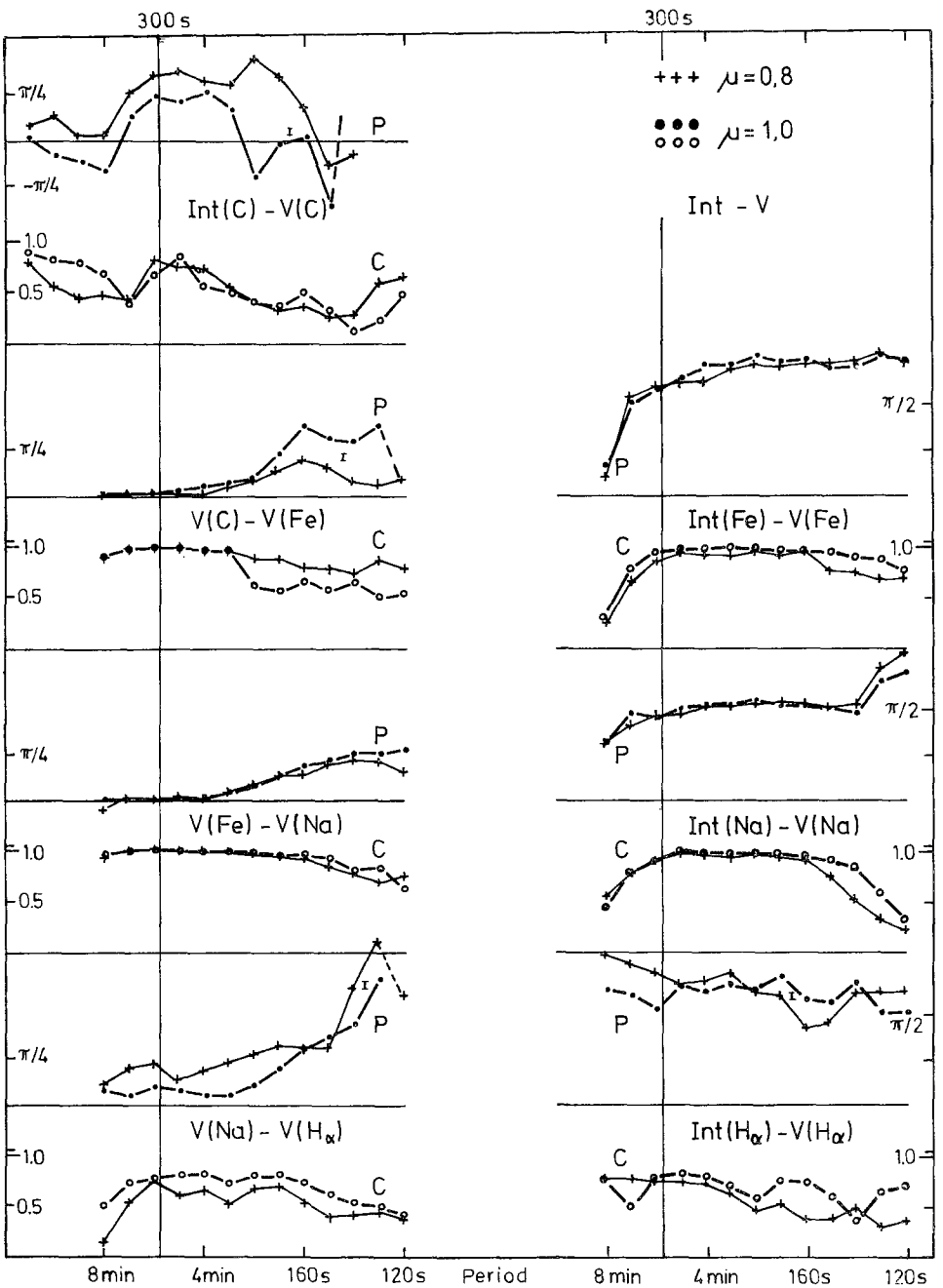

Fig. 7. Phase and coherence spectra ($P(\omega)$ and $C(\omega)$) of velocity and intensity fluctuations at different levels of the solar atmosphere. 80 % confidence limits are indicated by small vertical bars in the acoustic range. In the 300 s range the limits fall within the width of the drawn line.

important areas of the k, ω diagrams. First, we deal with the temporal phases which provide us with further information about the characteristics of propagation of monochromatic wave trains through different layers of the atmosphere. In Figure 7 we have plotted as a function of ω the phase differences (averages over $k = 0.0$ to 2.2 Mm^{-1}) between the v-fluctuations in the four spectral lines, and in the same way the time delays between intensity and velocity fluctuations observed in the same line.

At the resonance frequencies we observe only small but definitively positive phase lags between the velocity fluctuations of consecutive layers ($\Delta\varphi \leqslant 5°$), with exception of H$\alpha$, which lags about 10° to 20° behind NaD_1. This corroborates the theoretical picture (Moore, 1973) of an evanescent wave which by the effect of weak dissipation in the upper layers obtains a finite vertical phase velocity.

The intensity in the line (derived from the same part of the profile as the velocity) precedes the upward motion by about 40° in C I, and by 80° to 105° in the other spectral lines – in agreement with earlier observations. Again, this phase relation is precisely what theory predicts for evanescent waves. There is a rapid increase of the phase angle up to 125° and 135° at higher frequencies in the Fe I line which is remarkable in comparison with the sodium line which retains a constant value of 90° to oscillation periods as low as $T \approx 140$ s, whereas in other respects such a comparison yields only minor quantitative differences among these two lines.

We want to point out that *no* significant change of the phase relations with the wavenumber has been found in the range used for averaging.

The low frequency part of the phase spectra has only been investigated in the C I line, where convective motion can still be observed well enough. Here we find the upward motion leading brightness by ≈ 40 s on the average. However, if we do not average the whole range from 0 to 2.2 Mm^{-1}, but rather separately in five successive domains each one covering a range in k of 0.44 Mm^{-1} (cf. inset of Figure 8), a conspicuous dependance of the phase on wavenumber is found. The lead of some 50 s of the upward motion gradually decreases towards higher wavenumbers and finally becomes a lag of about 60 s at wavelengths smaller than 2″.4. From the point of view of hydrodynamics a reason for this change in the sign of the phase is not obvious. It is conceivable that the change of phase is due to a similar change in the brightness distribution as a function of cell diameter: The photospheric granulation pattern consists of bright cells with dark borders (downward motion being well correlated with low brightness), whereas the large convective cells (supergranulation) appear in low photospheric layers with *bright* borders, as a consequence of the influence of magnetic fields concentrated at the borders on the energy transfer.

This hypothesis, however, does not explain the high coherence at an intermediate cell size, where the phase drops to zero. A second hypothesis, which also accounts for the gradual change of the phase, appears rather speculative at the moment. We assume that in the smaller cells we observe a relatively large fraction of the 'active' convective layer, in comparison with the larger elements of which we observe probably only the upper 'skin' carried along with the cellular motion. We therefore see this motion already some time before the source becomes visible. Furthermore, the low absolute

velocities observed in large convective cells ($V_{\max,\mathrm{SG}}/V_{\max,\mathrm{GR}} \approx \frac{1}{4}$) combined with the comparatively strong horizontal component of the flow

$$(v_{\mathrm{hor}}^2/v_{\mathrm{vert}}^2)_{\mathrm{SG}} \approx 10\,; \quad (v_{\mathrm{hor}}^2/v_{\mathrm{vert}}^2)_{\mathrm{GR}} \leqslant 2\,,$$

spreading the energy more efficiently in the horizontal direction, would cause the temperature excess to become visible only after the motion. Off the center, the v-fluctuations of the larger elements mainly come from the prevailing horizontal component of the velocity field. Accordingly the resulting random phase differences at low wave numbers cancel each other and the coherence is reduced below 0.50.

At periods $T < 190$ s the differences in phase among the four different lines increase rapidly and obtain values in between 40° and 120°. Since this is the domain of propagating acoustical waves ($\omega_a = 2.9 \times 10^{-2}\ \mathrm{s}^{-1}$), we may assume that phase velocity and group velocity are nearly equal (this assumption is justified by recent observations of the vertical propagation of individual prominent disturbances (Deubner, in preparation), which gives us an excellent means of estimating the height of the line-forming layers within a geometrical scale). Thus, the following relative heights are obtained successively:

C I (5380) 0 km,
Fe I (5383) 200 km,
Na I (5896) 320 km,
Hα (6563) (700–800 km).

The value of Hα is suprisingly low and is probably not truly representative of the height of the line-forming layer due to radiation transfer effects. Theoretical estimates given by Schoolman (1972), however, do agree roughly with this value. A more detailed investigation of this subject is presently undertaken and will be published separately.

One dimensional phase spectra have been computed as a function of k from a set of spectrograms selected from the same material used throughout this paper by choosing only those 10% (i.e. 32 spectrograms) with the highest average rms velocity fluctuations in the horizontal wavelength range from 1″ to 3″. In performing the numerical computation, taking full advantage of the high spatial resolution of the spectrograms, phase and coherence have been calculated to the limit of the Nyquist frequency at $k = 16\ \mathrm{Mm}^{-1}$. The spectra show the relative spatial distribution of brightness and velocity patterns in the different layers observed (Figure 8).

As expected, upward motions and bright elements are well correlated in the photosphere (C I), the basic structure of the velocity pattern still being the same in the Fe I line, whereas in Na I the coherence decreases rapidly already at low wavenumbers. Elements smaller than 2″.5 are essentially uncorrelated to the photosphere, with the exception of a small wavenumber band at $10\ \mathrm{Mm}^{-1}$ (≈0″.9), where again some positive correlation is observed. The source of this effect can easily identified

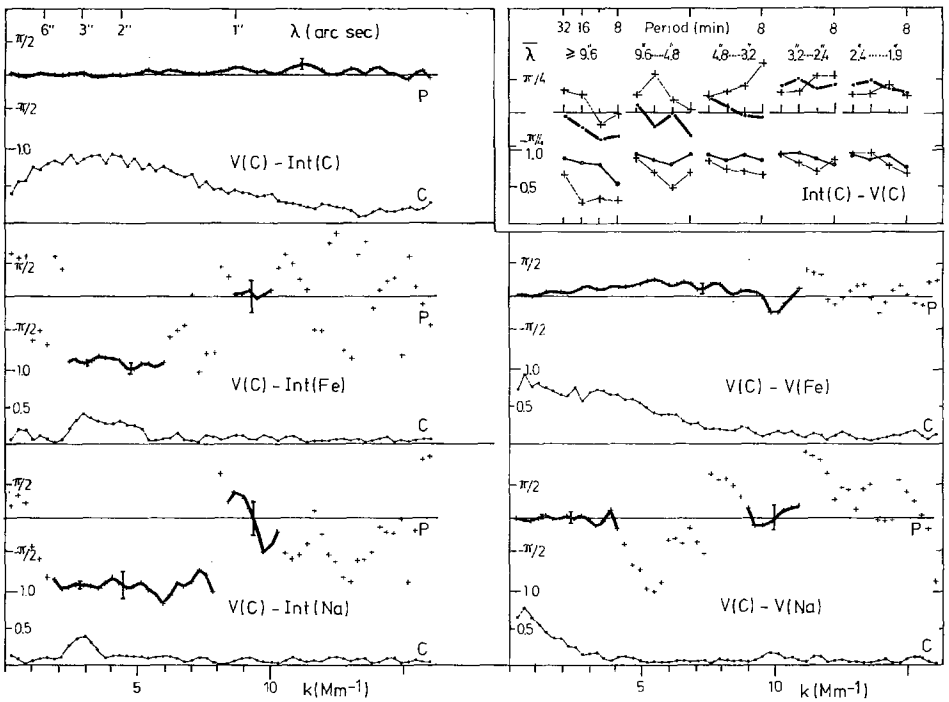

Fig. 8. Phase and coherence spectra $P(k)$ and $C(k)$ computed from a selected set of highest quality spectrograms taken at the center of the disk. Vertical bars indicate the 80 % confidence limits. Inset: Phase and coherence spectra $P(\omega)$ and $C(\omega)$ for low frequencies of fluctuations in the C I line computed separately in five consecutive wavenumber ranges.

in the solar spectrum with the position of bright granules, which quite commonly show in the Na I line a prominent spike-like excursion toward the blue.

The picture emerging from the brightness fluctuations appears more complicated: In the two upper lines these fluctuations are anti-correlated with the velocity field of the photosphere for element sizes comparable to the granular scale (2 to 7 Mm^{-1}). This effect has been reported first by Evans and Catalano (1972) and later also by Canfield and Mehltretter (1973), who interpreted the observed anticorrelation as a consequence of convective overshoot. But again, at wavenumbers from 9 to 10 Mm^{-1} the phase switches back to values grouping around zero degrees. This can only mean, if one trusts at all in phase values with a coherence as low as 10%, that occasionally small energetic convective elements succeed in penetrating to the lower chromosphere without loosing their identity. Probably the magnetic field as a guiding or channeling frame is of importance in this process. Further high resolution observations are necessary to study this effect in detail.

4. Discussion and Concluding Remarks

Since in the preceding chapter results which are not directly related to the 5-min

oscillations have been discussed already, we now turn to the questions raised at the beginning.

This investigation has confirmed again that the oscillations with periods from 240 to 300 observed in the photosphere and lower chromosphere are 'evanescent waves' driven from layers below the photosphere. The phase spectra indicate that these waves have a finite phase velocity directed upward in the atmosphere. This points to dissipation processes occurring already in the photosphere. The amount of dissipation from oscillations has been estimated by Canfield and Musman (1973). They have shown, that a significant part of the radiative losses of the chromosphere may be contained in the energy dissipated by the 5-min oscillations. The diagnostic diagrams do not exclude the possibility that some fraction of the oscillatory energy reaches the upper layers in the mode of progressive sound waves which can dissipate there more efficiently. Another component of the sound waves observed in the chromosphere is generated independently of the oscillations immediately by visible convective processes in the photosphere. Furthermore, we were able to confirm that the maximum of the energy distribution of the oscillations is located at comparatively long wavelengths (9″–15″) and significant amounts of energy are probably present in still larger elements or wavelengths. From this large horizontal scale and from the comparison of the relevant time scales we have been lead to the conclusion that the oscillations cannot be excited by single granules. The concomitant observations of Stix and Wöhl which prove the absence of horizontal sound waves contrary to the predictions of theories of local excitation by granules are fully confirmed by our own k, ω diagrams. The coincidences of the brightening of granules with the initial phases of oscillations which have been reported by Evans and Michard (1962b) therefore require some independent explanation. The same kind of coincidence was observed by Deubner (1973) in the case of an exploding granule which produced some of the wave modes predicted by the local excitation theory, but no 5-min oscillations. It is very likely that Evans and Michard also have been observing similar events.

The omnipresence and homogeneity of the oscillatory velocity field renders a search for larger local sources of excitation futile, especially with regard to the energy contained in the frequency range crucial for driving the oscillations, which cannot be expected to be sufficient in larger elements because of their entirely discordant time scales. A global theory, based on the oscillatory instability of subphotospheric layers as developed in recent years by Ulrich (1970), Leibacher (1971) and Wolff (1972b) seems best suited to give an appropriate description of the phenomena observed, provided the theory also succeeds in explaining the preference for periods in the 300 s range out of a wide spectrum of possible propagating eigenmodes.

Acknowledgements

My thanks are due to J. W. Evans and the staff of Sacramento Peak Observatory for their hospitality and to the Joint Institute for Laboratory Astrophysics which provided the financial support for my stay at Sunspot. I gratefully acknowledge inspiring

discussions with C. Durrant, J. Leibacher, H. U. Schmidt, and J. Thomas. The lambda meter used for digitizing the spectra consisted of parts of the DESO project supported by the Deutsche Forschungsgemeinschaft. The numerical computations have been performed on the UNIVAC 1106 at the Rechenzentrum der Universität Freiburg.

References

Canfield, R. C. and Mehltretter, J. P.: 1973, *Solar Phys.* **33**, 33.
Canfield, R. C. and Musman, S.: 1973, *Astrophys. J. Letters* **184**, L131.
Clark, P. A. and Clark, A., Jr.: 1973, *Solar Phys.* **30**, 319.
Deubner, F.-L.: 1972, *Solar Phys.* **22**, 263.
Deubner, F.-L.: 1973, in R. Grant Athay (ed.), 'Chromospheric Fine Structure', *IAU Symp.* **56**, D. Reidel Publ. Co., Dordrecht-Holland, p. 185.
Deubner, F.-L.: 1974, *Solar Phys.* **36**, 299.
Edmonds, F. N. Jr. and Webb, C. J.: 1972a, *Solar Phys.* **22**, 276.
Edmonds, F. N. Jr. and Webb, C. J.: 1972b, *Solar Phys.* **25**, 44.
Evans, J. W. and Catalano, C. P.: 1972, *Solar Phys.* **27**, 299.
Evans, J. W. and Michard, R.: 1962a, *Astrophys. J.* **135**, 812.
Evans, J. W. and Michard, R.: 1962b, *Astrophys. J.* **136**, 493.
Fossat, E. and Ricort, G.: 1973, *Solar Phys.* **28**, 311.
Frazier, E. N.: 1968, *Z. Astrophys.* **68**, 345.
Leibacher, J. W.: 1971, Thesis, Harvard University.
Mattig, W. and Nesis, A.: 1974, *Solar Phys.* **36**, 3.
Mein, P.: 1966, *Ann. Astrophys.* **29**, 153.
Meyer, F. and Schmidt, H. U.: 1967, *Z. Astrophys.* **65**, 274.
Moore, R. L.: 1973, Big Bear Solar Observatory Report BBSO 0132a.
Schoolman, S. A.: 1972, *Solar Phys.* **22**, 344.
Stix, M.: 1970, *Astron. Astrophys.* **4**, 189.
Stix, M. and Wöhl, H.: 1974, *Solar Phys.* **37**, 63.
Tanenbaum, A. S., Wilcox, J. M., Frazier, E. N., and Howard, R.: 1969, *Solar Phys.* **9**, 328.
Thomas, J. H.: 1972, *Solar Phys.* **24**, 262.
Uberoi, M. S.: 1955, *Astrophys. J.* **122**, 466.
Ulrich, R. K.: 1970, *Astrophys. J.* **162**, 993.
Wolff, C. L.: 1972a, *Astrophys. J.* **176**, 833.
Wolff, C. L.: 1972b, *Astrophys. J. Letters* **177**, L87.
Wolff, C. L.: 1973, *Solar Phys.* **32**, 31.